CFD-based Flutter Analyses of the AWI high-aspect-ratio Wing Configuration

Reik Thormann*, Etienne Coetzee and Bernd Stickan

**Airbus Operations GmbH, Loads and Aeroelastics*
Airbus-Allee 1, 28199 Bremen
Germany

ABSTRACT

Within the Agile Wing Integration (AWI) project, a very flexible high-aspect-ratio wing (HARW) configuration was analyzed with special emphasis on nonlinear structures and their effect on aeroelastic stability and limit-cycle oscillations. The numerical investigations of the configuration, see Fig. 1, were complemented by experimental data obtained in the Airbus wind-tunnel facilities in Filton. In the current work, the classical p-k flutter process is extended for such models. Although the wind-tunnel is operated at low Mach numbers, CFD-based aerodynamics are used to account for the in-plane motion, inherently involved in analyses of HARW. The applied flutter process involves coupled CFD-CSM simulations using Nastran SOL400 to compute the structural deformations and DLR-TAU code for the aerodynamics. The LFD-TAU code is used to compute the generalised aerodynamic forces (GAF) using proper orthogonal decomposition (POD) to define the excitation. At the beginning of each velocity step within the p-k flutter solver, the modal frequencies and mode shapes are interpolated as well as the GAF which is projected onto the actual modes using the least-square approach. This rather complex process is necessary, since the shapes can vary significantly depending on the wing's loading, see Fig. 2. The obtained flutter-onset speeds are shown in Fig. 3 as function of the angle of attack depicting two mechanisms.

In the final paper, different effects of modelling assumptions onto the flutter results will be discussed. Moreover, the numeric results will be compared to the experimental wind-tunnel data. This will include comparisons of the static deformation in dependence of the flow conditions as well as frequency and damping curves.

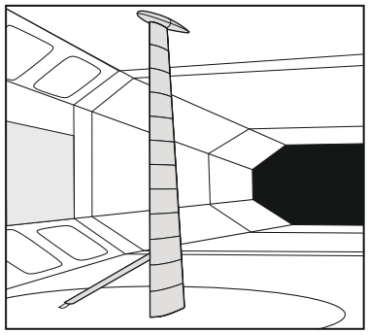

Fig 1: AWI wind-tunnel configuration

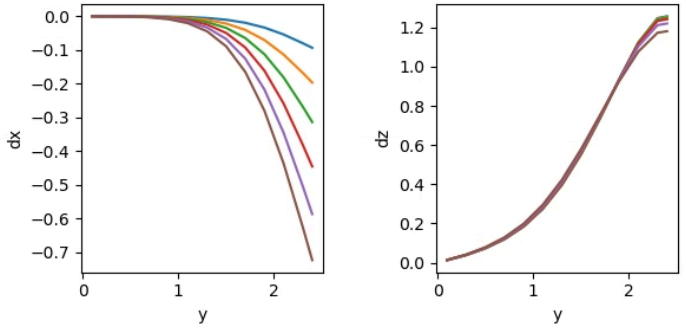

Fig. 2: Shape of first out-of-plane bending depending on the static aerodynamic loading

Fig 3: Flutter onset of:
1st in-plane and 1st out-of-plane bending (blue);
1st in-plane and 2nd out-of-plane bending (red)